Enhancements of the Mechanical Properties for Banana/Sisal Fibers by Cold Glow Discharge Oxygen Plasma Treatment

upendra sharan gupta (upendrasharangupta@gmail.com)
Shri Vaishnav Vidyapeeth Vishwavidyalaya https://orcid.org/0000-0002-7489-5068
Sudhir Tiwari
Uttam Sharma

Research Article

Keywords: Banana fiber, Sisal fiber, Natural fiber, Mechanical Properties, adhesion, cold glow discharge oxygen plasma treatment, Natural Fibre composite

Posted Date: April 18th, 2022

DOI: https://doi.org/10.21203/rs.3.rs-1544848/v1

Abstract

Banana fiber is a natural byproduct of the pseudostem processing of the "banana plant" (Musasepientum). Agave sisalana is a rosette-forming succulent plant used for its fibers, despite difficulties like hydrophilicity and performance swings, sisal fibers were cheap in compactness, generally accessible, and environmentally benign. In this investigation, the effects of different plasma powers (80W and 120W) for 30 minutes on mechanical and surface characteristics of unidirectional banana and sisal fibers surface treated with cold glow discharge oxygen plasma were investigated. The banana-sisal fiber reinforced epoxy composite (BSFREC) had nearly 90.44 percent higher interlaminar shear strength, 132.27 percent greater flexural strength, 50.0 percent higher larger elongation break, and 115.155 percent higher tensile strength as evaluated towards an untreated banana-sisal fiber-reinforced epoxy laminate. The morphological characteristics of cold glow discharge oxygen plasma-treated banana and sisal fibers were compared to pretreatment banana and sisal fibers using FT-IR spectroscopy and (XRD), revealing an improvement in fiber surface structure. Physical treatment of fibers boosts their adherence to the matrix. Banana and Sisal fibers may be employed in industrial applications after being surface-treated, making them an efficient and promising material that contributes to the world's goal of supporting natural resources that are sustainable and recyclable.

1. Introduction

Environmental issues such as soil and water contamination, garbage disposal, and environmental efficiency gains are driving the creation of greener materials [1]. Innovators focusing on fiber-reinforced polymeric composites are appealing to bio-renewable bio-based fibers to create and being used in this context[2] Researchers are looking into cellulosic fibers as a continuous or intermittent substitute for petro synthetic fibers, that were neither recyclable nor biodegradable, as a consequence of rising concern and awareness about the environment [3]. The emerging need for greener environments had prompted the development of environmentally friendly materials and the efficient use of natural resources. As a result, there is a burgeoning need for high-performance manufactured items made from natural renewable resources. Laminates are flexible, high-performance materials with mechanical and thermal capabilities hard to attain in a single material. Fiber-reinforced laminate is a ground-breaking material with a plethora of applications. Biopolymer fiber composites were stated to be used in several industries, including building, furniture, and maritime applications [4–6]. The development of innovative fiber-based materials has already demonstrated their enormous potential for increasing human life quality in recent decades. These fibrous materials contain both natural and man-made ingredients. Natural fibers provide numerous advantages over carbon-reinforced fibers. They are environmentally sustainable, abundant, inexhaustible, durable, resource, biocompatible, small and simple, toxicological, and easily intervened, all while consuming low energy [7–9]. Lignocellulosic fibers are among the most researched because they offer tremendous strength at modest weight loads that are inevitably the foremost common in the environment. The hydrophilic characteristic of natural fibers, on the other hand, is a major hindrance to their use as reinforced composites. Low moisture friction in natural fibers induces incompatibilities and

poor permeability with hydrophobic polymers, causing contact interactions at the fiber/matrix interfaces to be disrupted [9–10]. Many surface engineering approaches, such as chemicals and plasma processes, have been examined for natural fibers to enhance the fiber-matrix outcomes for polymer laminates. The most extensively employed chemical modifications with plant fibers utilized to strengthen thermoplastics as well as thermosetting polymers are alkaline treatment [11–12], silane treatment [12–13], and acetylation treatment [11, 14]. While chemically treated fiber surfaces have increased interfacial adhesion to some extent, environmental concerns such as chemical recycling after treatment, as well as the high cost of chemical treatment, remain unsolved. Different treatments would be used to remove lignin, hemicellulose, lubricants, hydrocarbons, and other low molecular weight substances [15]. Owing to increasing concerns about environmental pollution, different chemical treatments have not been widely employed in the industry in recent years [16]. Alternative technologies have included the low-temperature plasma approach. This method has also been employed to improve the texture of fibers in a modest but effective way [17]. Besides introducing positively charged or energized clusters or even a new polymer surface capable of forming a stable complex among the fiber along with the matrix, as well as exfoliation surface of the fibers to boost structural interlocks of both the fiber and the matrix, plasma treatment significantly increased fiber-matrix adhesion. Plasma treatment allows impurities and weakly attached films to be removed, wettability to be improved by integrating polar present on the surface, and absorption bands to be formed, allowing for bond formation [18,19]. Plasma treatment frequently involves the use of chemically inert, reactive, and non-polymerizable gases, as well as reactive and polymerizable gases [20]. Plasma treatment had been utilized to strengthen the surface of sisal fibers to boost cohesiveness between the reinforcing material, sisal fibers, and PP, a fiber composite matrix. Fiber extraction from plasma-treated fibers necessitates a significantly higher level of stress than fiber extraction from untreated fibers. Several adjustments were performed for the same specimen size based on the single fiber tensile test results[21].To investigate changes in water removal induced by an oxygen plasma alteration, woven-type basalt fibers with a cold oxygen plasma atmosphere were used [22]. The elastic modulus of Ramie fiber increased during plasma treatment, culminating in a stiffer fiber[23]. Argon plasma was created using a revolutionary technique known as "pad dry plasma cure."According to the investigation, treating the "bridging agent as well as cellulose molecules with Argon plasma might assist improve its bridging action."Argon plasma treatment improved tensile characteristics and elongation % considerably[24]. Kamlangkla et al. treated cotton fabrics with sulphur hexafluoride (SF_6), an easily available and inexpensive fluoro-containing gas. Plasma treatment considerably enhanced the water-resistance and wettability of nonpolar polymers in cotton fabrics, allowing for easier cohesive bonding. [25]. For plasma treatment of cotton and wool, the "polymerizable plasma gas hexafluoroethane" and the "non-polymerizable reactive plasma gas oxygen" were used. The structure and chemical composition of the fiber surface in cotton and wool textiles were both enhanced as a consequence of the research [26]. The effects of chitosan treatment and low-pressure pseudo-discharge oxygen plasma on wool coloring characteristics were investigated by Gawish et al.When compared to untreated wool materials, oxygenated plasma-enhanced wettability, hydrophilicity, and dyeability[27]. Ebru Bozaci et al. employed atmospheric glow discharge plasma to treat jute. Following the alkali treatment, the jute fibers were treated with plasma, which resulted in several morphological features.

Surface quality and wickability improved as plasma power and process parameters were enhanced [28]. The application of cold glow discharge oxygen treatment on banana as well as sisal fibers was investigated in this study. Throughout this investigation, unidirectional banana and sisal fibers were surfaces treated with cold glow discharge plasma oxygen, as well as the influence on mechanical characteristics was consistently evaluated. To enhance the combination of banana and sisal fiber with epoxy resin, oxygen plasma treatments were utilized to change the surface of the banana along with sisal fibers at different plasma energies of 80 W and 120 W for 30 minutes. The mechanical performance of pre-treated and cold glow discharge oxygen plasma modified banana, as well as sisal fibers, was evaluated, and ILSS was utilized to assess interfacial bonding of composites (interlaminar shear strength. The ultimate tensile strength, % elongation, force-displacement, single fiber tensile test, fiber diameter, and flexure tests were also evaluated. X-ray Diffraction had been acquainted to explore the macromolecular morphology of untreated and treated banana and sisal fibers, as well as the change in crystallinity during cold glow discharge oxygen plasma treatment (XRD). Fourier transforms infrared spectroscopy (FT-IR) had been employed to examine "surface microstructural and fiber surface chemistry."

2. Materials And Methodology

2.1 Fiber and Matrix Materials

During this investigation, banana and sisal fibers have been employed as reinforcement, employing epoxy Lapox Metalam- B as the matrix. The banana, as well as sisal fiber, were furnished with Go Green product Alwarthirunagar Chennai. Lapox Metalam - B epoxy was utilized as the matrix, with Lapox Metalam - B also serving as the hardener and resin binder.Atul Industries Gujrat in India provided Lapox Metalam B (Viscosity at 25°C: 800–1,200 MPa, Density 1.00–1.20 g/cm^3) and Lapox Metalam B Hardener (Viscosity at 25°C: 300–600 MPa, Density 0.95–1.00 g/cm^3).

2.2 Cold Glow Discharge Oxygen Plasma Treatment of Banana and Sisal Fibre

Shri Vaishnav Vidyapeeth Vishwavidyalaya, Indore's Centre of Excellence for Plasma Research, has developed, built, and deployed a system for creating Glow Discharge plasma employing RF and DC electricity. In the plasma system, a cylindrical stainless steel vacuum chamber (stainless steel material (SS304)) is employed. A typical plasma treatment system is depicted in Fig. 1, which includes a "vacuum chamber" with a capacity of 30 liters, a height of 300 mm, and a diameter of 360 mm, as well as a cathode-electrode unit (02 round electrodes, one of which has a movable displacement, referred to as the "anode," and a fixed electrode, referred to as the "cathode"). A high voltage DC-power supply (2 KV, 1 amp) for the DC electric discharge of gas and an RF power supply (SEREN RF Generator) with 13.56MHz, 600 Watt, and an automated matching network for RF electric discharge of gas. Gas is used to create incandescent discharge plasma. To empty the container, the gadget combines a rotary pump (CG COMMERCIAL MOTORS) and a turbo molecular pump (Pfeiffer Vacuum, Germany)."To support the

TurboMolecular Pump, a rotating pump (RP) was incorporated, with a pumping speed of 60 L/s."The reactor provides an ultimate vacuum of $1x10^{-6}$ mbar when all outputs are bleeped. A rotating pump is used to pump gas supplying connections across locations. Independent gas valves separate all cross-functional and cross lines to the gas cylinders, flow controllers, and vacuum chamber. A digital Pirani gauge is routinely used to monitor vacuum from the ambient pressure, and an Ion gauge (PFEIFFER VACUUM) is used to measure vacuum within the chamber from 10^{-3} mbar to 10^{-9} mbar. A mass flow controller (EVN 116 metering valve, Dosing Valve) is a device that accurately regulates the gas flow.

As shown in Fig. 2, banana and sisal fibers were modified employing Cold Glow Discharge Oxygen Plasma treatment using RF-plasma systems at 80W (30 min) and 120W (30 min).To begin, compressed air was used to clean the inside of the chamber glass tube and the sample container. For both the "positive and ground electrodes," the substrates (40 grams of fibers) are being weighed accurately in the vacuum chamber. The oxygen gas was then fed into the chamber through a "Dosing valve" at a flow rate of 100 mbar lit/s until the vacuum reached almost "$1x10^{-1}$ millibars" and then RF power was provided to the electrodes after an automated matching network, resulting in an oxygen plasma with zero watt reflection. Before obtaining optimal, we experiment with all of the factors, such as power, time, and flow rate. We acquired satisfactory results utilizing banana and sisal fibers after "30 minutes at 80 Watt and 30 minutes at 120 Watt."After the treatment had finished removing any undesirable reactive compounds, the gas flow was continued for another 10 minutes. The treated fibers were maintained in a vacuum-sealed envelope after being taken from the holder for various investigations.

2.3. Composite preparation

Banana and sisal fibers are being trimmed to a 170-mm length. A hand lay-up approach was employed for reinforced hybrid composites. The matrix material was Lapox Metalam B (Viscosity at 25°C: 800–1,200 MPa, Density 1.00–1.20 g/cm^3), with the resin binder being Lapox Metalam B Hardener (Viscosity at 25°C: 300–600 Mpa, density 0.95–1.00 g/cm^3).To create the composite, epoxy resin was mixed with a 2:1 ratio of hardener. The matrix was created using this solution. A metal frame was being used to cover the mold, as well as the plastic sheet, which was coated with silicone spray, allowing for quick removal and a high surface finish in the laminates. By brushing and pressing with the roller, the resin was equally dispersed throughout the entire area of each surface, and any air gaps were filled. Hybrid laminates with a volume fraction of 50% banana fiber and 50% sisal fiber were produced at different fiber loadings (10–40% volume fraction) while maintaining the volume fraction of banana and sisal at 1: 1. EBESEBESEBES had been used to stack the epoxy and fiber layers (E-Epoxy, B-Banana, and S-Sisal). The fiber orientation was kept at 0 °. The laminates have been extracted from the mold and were cured at ambient temperature. Under a 60 kg load, the castings of each composite were cured for 24 hours. The dimensions of the composites were cut with a diamond cutter in compliance with ASTM standards. The composites were firm and dry enough to cut after the curing step.

2.4 Mechanical Characterisation of composite

The tensile specimen is made with an "ASTM D3039-00 computerized universal testing machine (UTM TUE-C-200/200 kN)" with a cross-head speed of 5 mm/min and dimensions for 165 mm x 19 mm x 3 mm and a notch circle radius of 76 mm. The flexural evaluation was performed in accordance with ASTM-D790 utilizing a Digital Tensile Testing Machine (KMI-1.3 D)/2.5 kN with a sample size of 125 mm x 12.7 mm x 3 mm and a cross-head speed of 5 mm/min. To assess ILSS results according to ASTM D-2344, a Digital Tensile Testing Machine (KMI-1.3 D)/2.5 kN with a cross-head speed of 5 mm/min as well as a nominal 5:1 span-to-depth ratio was employed. Each specimen measured 6.4 mm in breadth and 26.3 mm in length. Three samples were taken for each measured reading, and the average findings of the analyses were recorded.

2.5 Morphological Analysis of Fibers

2.5.1 Single fiber pull out test of Banana and Sisal fiber

The tensile test sample preparation and testing procedures were performed in compliance with the ASTMC1557-03 standards [29]. During the tensile test, the fibers were clamped inside the testing machine's jaws, which was performed on a "Digital Tensile Testing Machine (KMI-1.3D/2.5kN) template" [30]. The cross-sectional area of cold glow discharge plasma oxygen treated and untreated banana and sisal fiber was assessed using a Polarising projection microscope (Innolab RPL-4,17204 with 10 X Magnification), which would have been required for measuring sample mean diameter. At least ten measurements were taken. More than 30 fibers were examined for each cold glow to ensure that more than 10 exact readings were collected.

2.5.2 Surface characterization of untreated and cold glow discharge oxygen treated banana and sisal fiber by using FTIR

The impact of various physical treatments on the surface properties of fiber as support for interfacial bonding was investigated using FTIR analysis. To examine the materials, an attenuated total reflectance device in a twin beam "FTIR spectrophotometer (SHIMADZU FTIR-8900 spectrophotometer) with a resolution of 2 cm^{-1} in the wavenumber range of 4000 – 400 cm" was utilized. On average, 25 scans were acquired.

2.5.3 Surface characterization of untreated and cold glow discharge oxygen treated banana and sisal fiber by using XRD

The X-ray diffractograms for cold glow discharge plasma oxygen treated banana and sisal fiber and pretreated banana and sisal fiber were obtained on the "image plate (Mar 345 dtb) area detector of Indus-2 Angle-Dispersive X-ray Diffraction (ADXRD) Beamline (BL-12)" utilizing calibrated photon energies (17.42111 keV).

3. Results And Discussion

3.1 Ultimate Tensile Strength and % Elongation Characterisation

Figures 3 and 4 reveal that an untreated banana sisal fiber-reinforced epoxy laminate's maximum tensile strength and % Elongation break have been 56.35 MPa and 4.6 mm, respectively. A pretreatment banana-sisal fiber-reinforced epoxy laminate with a volume percent of fiber of 40% produced the best mechanical properties, including tensile strength 56.35 MPa and 4.6 mm, and percent Elongation break attributes. "Improved matrix-fiber cohesion improves the mechanical characteristics of the natural fiber-reinforced laminate significantly." [31,32]. Figures 3 and 4 exhibits the cold glow discharge plasma-treated banana-sisal fiber-reinforced epoxy laminate's maximum tensile strength and % Elongation break. Cold glow discharge plasma oxygen is being used to treat the surface of banana and sisal fibers at power levels of 80 W (30 min) as well as 120 W (30 min), and the treated fibers have been used to create composites. Percentage of tensile strength after cold glow discharge plasma oxygen treatment of banana and sisal fiber with plasma powers of 80 W (30 min) and 120 W (30 min), the elongation break of banana- sisal fiber-reinforced epoxy laminate rose to 121.24 Mpa,6.9 mm and 113.47 Mpa,6.8 mm, respectively.This corresponds to gains of around 115.155%, 50.0%, and 101.366%, 47.82%, respectively. Up to 10% volume of fiber, tensile strength, and % Elongation Break grew consistently, with the trend continuing at 40% volume of fiber. Mechanical attributes are strengthened to some extent when the volume percent is enhanced. The topography of the surface becomes rough as hemicellulose, lignin, waxes, and pectin are removed. The fiber bundles were also separated into smaller fibers, the fiber diameter was reduced, and the aspect ratio was enhanced. The O-H and C-OOH groups on the fiber surface are exposed when waxy substances dissolve, resulting in increased polarity and decreased acidity of the fiber's surface topography. Surface functional groups are linked by interactions between energized plasma species and the substrate surface, whereas surface bridges are typically created by reactions between excited surface species.[33,34].

3.2 Flexural Test

Figure 5 depicts the flexural strength of pretreated and cold glow discharge plasma oxygen treated banana-sisal reinforced epoxy composites with various fiber percentages. The highest flexural strength (32.25 MPa) was reached with a 40% volume of untreated banana-sisal reinforced epoxy composite, while the lowest was achieved with a 10% volume of untreated banana-sisal reinforced epoxy composite (16.63 MPa). Flexural strength normally increases as fiber loading increases. The enhanced cohesiveness between matrix and fiber enhanced the mechanical properties of the natural fiber-reinforced laminate substantially.[35] At different power levels of 80 W (30 min) and 120 W (30 min), 40 percent volume of banana-sisal fiber loading, the flexural strength for the fiber-reinforced cold glow oxygen laminate increased by nearly 132.27% and 124.34%, respectively, when compared to the untreated banana-sisal reinforced epoxy laminate. Plasma treatments may have a significant influence by eliminating organic contaminants from the surface, removing the poor boundary layer and extending contact area, reinforcing the surface layer, and modifying the chemical structure.[36,37]

3.3 Interlaminar Shear Strength (ILSS)

The interlaminar shear strength of banana-sisal reinforced epoxy composites treated with cold glow discharge plasma oxygen is shown in Fig. 4. According to the ILSS investigations, the ILSS of cold glow discharge plasma oxygen treated banana-sisal reinforced epoxy laminates enhances to 80 W (30 min) at 40% vol. fiber.When compared to untreated banana-sisal reinforced epoxy composites, the ILSS values for cold plasma oxygen treated banana-sisal reinforced epoxy composites with plasma powers of 80 W and 120 W rise by 90.44% and 73.98%, respectively. Plasma treatments chip away at cellulose and hemicellulose more readily as they become more susceptible to plasma, enhancing cohesive adhesion [38].

3.4 Force- Displacement Curve

As shown in Fig. 7(a-c), tensile tests have been used to plot force vs. displacement graphs for untreated banana-sisal reinforced epoxy composites and cold glow discharge plasma oxygen treated banana-sisal reinforced epoxy composites with 20%, 30%, and 40% vol. of fiber, demonstrating that maximum force carrying capacity increases as fiber content in epoxy matrix increases. The influence of plasma power on banana-sisal fiber force-displacement graphs was examined using composite force-displacement data. When banana-sisal fiber is treated with cold glow discharge plasma oxygen at 80 W for 30 minutes, the load increases gradually until it approaches the material's maximum load-carrying capability at 40% fiber volume, at which point it gradually drops. Figure 7(a) shows how to follow the linear path of force-displacement graphs up to a load of 6911.8 N. The ultimate point on the force-displacement curve (ultimate load 14870.87 N) shows the total full rupture of the polymer composite throughout the composite when the banana-sisal fiber is treated with cold glow discharge plasma oxygen at 80 W. (30 min). When the banana and sisal fiber is exposed to cold glow discharge plasma oxygen for 30 minutes at 80W and 120W, the force-displacement graph is followed linearly up to loads of 14870.87N and 13917.0 N, respectively. Employing plasma powers of 80 W and 120 W, cold glow discharge plasma oxygen treated banana-sisal reinforced epoxy composites exhibited rising force (N) values of 115.15% and 101.36%, respectively. The load is spread equally over the fiber and matrix in the linear curve. The fibers of the material begin to emerge as the bends decrease. The cohesive bonding among the fiber as well as the matrix has been identified as the most critical variable in predicting the tensile strength of banana-sisal and epoxy composites.

3.5 Single Fibre Pull Out Test

Table 1 illustrates the average fiber diameter, breaking load, ultimate tensile strength, and % elongation characteristics of untreated and cold glow discharge oxygen treated banana and sisal single fibers. To ascertain whether the cold glow discharge oxygen plasma modification of banana and sisal fiber affects the strength of the treated fibers. After cold glow discharge plasma oxygen treatment of banana fiber with plasma intensities of 80W(30 min) and 120 W(30 min), the breaking load, tensile strength, and percent elongation break are 3.52N,53.31 Mpa,11.6 mm, and 3.18N,31.25 Mpa,9.1 mm, respectively. After cold glow discharge plasma oxygen treatment with plasma intensities of 80 W (30 min) and 120 W (30 min),

the breaking load, tensile strength, and % elongation break of sisal fiber are 4.14 N,72.344 Mpa,12.1 mm, and 3.76 N,46.775 Mpa,11.2 mm, respectively. The accessibility of the fiber has enhanced as a result of the formation of cracks and grooves during the plasma treatment [39]. Plasma treatment improves textile structures by altering yarn and textile physical characteristics and creating micro pits on fiber surfaces [40-42].

Table 1
Influence of cold glow discharge plasma oxygen modification on fiber diameter, breaking load, tensile strength and % elongation of pretreated as well as cold glow discharge plasma oxygen treated banana and sisal fibers

Samples	Fiber diameter (μm)	Breaking Load(N)	Tensile Stregth in (MPa)	% Elongation (mm) (50mm Gauge length)
Untreated Banana fiber	420	2.54	18.34	8
Cold glow discharge plasma oxygen treated banana fiber 80 W (30 min)	290	3.52	53.31	11.6
Cold glow discharge plasma oxygen treated banana fiber 120 W (30 min)	360	3.18	31.25	9.3
Untreated Sisal fiber	450	3.14	19.753	9
Cold glow discharge plasma oxygen treated Sisal fiber 80 W(30 min)	270	4.14	72.344	12.1
Cold glow discharge plasma oxygen treated Sisal fiber 120 W (30 min)	320	3.76	46.775	11.2

3.6 Fourier Transform Infrared (FTIR) spectroscopy

Chemical characteristics, as revealed via Fourier Transform Infrared (FTIR) spectroscopy, establish the ability for most materials to execute a specific function, allowing for the examination of surface composition and/or interactions at composite material interfaces.[43,44].The FTIR spectrum of pretreated banana fiber is depicted in Fig. 8(a). This graphic illustrates the peak positions of peaks in the spectra from 4500 to 400 cm^{-1}. The valence vibrations of hydrogen-containing C–H along with O–H functional groups linked in carbohydrate and alcohol compounds found in untreated banana fibers, i.e. cellulose, hemicelluloses, and lignin, are related to the broad intensive peaks along with the zone of 4000–3500 cm^{-1} as well as 2900–2350 cm^{-1}, as well as the medium at 3350–2900 cm^{-1} [45–47]. Strong bands extending from 2350 to 1750 cm^{-1}, 1750 to 1650 cm^{-1}, and 1650 to 1450 cm^{-1} are linked with stretching vibrations in aromatic hydrocarbons' C = O and C = C groups, as well as ketone and aldehyde molecules. Although cellulose is liable for aldehyde compound vibrations [43], these peaks have been attributed to ketone components found in hemicelluloses and aromatics found in lignin, which have higher reflectance intensities in these wave number areas than cellulose-related compounds [45,46].

Untreated banana fiber has a greater intensity peak with regions of 2300–1650 cm^{-1} as well as 1750–1650 cm^{-1}, which can be attributed to the presence of more hemicelluloses, lignin components, and other components. The sequence of peaks registered with the fingerprint region between 1450 and 400 cm^{-1} is caused by the C–C and C–O identified in phenol, alcohol, and aromatic compounds, with lignin having the highest intensities between 1400 and 1200 cm^{-1} and cellulose and hemicellulose having the highest intensities among 1200 and 900 cm^{-1}[45,46]. Figure 8(d) illustrates the FTIR spectrum of pretreated sisal fiber. The various peaks with absorbance bands ranging from 4500 to 400 cm^{-1} were displayed within this image. Its broad, intense peaks in the 4000–3500 cm^{-1} and 2900–2350 cm^{-1} regions, as well as the medium at 3350–2900 cm^{-1}, were linked to "valence vibrations for hydrogen-containing C–H and O–H functional groups" found in carbohydrate and alcohol compounds found in untreated sisal fibers, particularly cellulose, hemicelluloses, and lignin.[48,49].Strong bands extending from 2350 to 1750 cm^{-1}, 1750 to 1650 cm^{-1}, as well as 1650 to 1450 cm^{-1} have been ascribed to stretching vibrations inside the C = O and C = C groups of aromatic hydrocarbons, as well as ketone and aldehyde molecules. Although aldehyde compound vibrations are induced via cellulose [50], all such peaks have been correlated to ketone and aromatic compounds found in hemicelluloses and lignin, which have higher reflectance intensities in these wave number zones than cellulose-related compounds [50,51]. The presence of more hemicelluloses, lignin components, and other components in untreated sisal fiber seems to have a higher intensity peak in sections of 2300–1650 cm^{-1} as well as 1750–1650 cm^{-1}. Identical peaks have been linked to ketone and aromatic compounds found in hemicelluloses and lignin, which have higher reflectance intensities in these waves number domains than cellulose-related compounds [50,51], despite the fact that cellulose has aldehyde compound vibrations. Due to the inclusion of extra hemicelluloses, lignin components, and other components, pretreated sisal fiber seems to have a higher intensity peak including regions of 2300–1650 cm^{-1} and 1750–1650 cm^{-1}. The C–C and C–O in phenol, alcohol, and aromatic compounds produce a sequence of maxima in the fingerprint zone between 1450 and 400 cm^{-1}, with lignin having the highest intensities in the range 1400–1200 cm^{-1} and cellulose and hemicellulose having the highest intensities in the range 1200–900 cm^{-1}[48–51].The FTIR spectra of banana fiber were altered after plasma treatment, as shown in Fig. 8(b),8 (c). Cold plasma oxygen treatment of banana fibers at 80 watts for 30 minutes and 120 watts for 30 minutes produced similar results.The decrease in intensities in the ranges of 2300–2200 cm^{-1} and 1900–1800 cm^{-1} as the values of plasma treatment parameters increase is primarily due to the reduction of aromatic and ketone compounds associated with bulk cellulose absorption from fibers[47], as well as the decrease in spectra intensity at 1550 cm^{-1} [47]. The most prominent alterations were detected when banana fiber was treated with cold plasma oxygen treated 120 W (30 min), demonstrating that the higher the treatment parameter values, the more substantial the changes. Figure 8(e),8(f) shows the FTIR spectra of sisal fiber after plasma treatment. Cold plasma oxygen at 80 W for 30 minutes and 120 W for 30 minutes had a significant effect on sisal fibers. The spectra at 3050 and 2840 cm^{-1} exhibit the "C-H bending vibration for hydrocarbon clusters," which is a distinguishing feature of both lactic and glycolic acids. Between 3050 and 2840 cm^{-1}, there is a considerable decrease in intensity and peak heights, "matching to CH_2 and CH_3 in lactic as well as

glycolic acids."The amplitude is approximately 1675 – 1600 cm^{-1} due to absorption bands of the carbonyl (C = O) group, which is an attribute of cellulose and hemicellulose. The amplitude along with apex height around the "carbonyl group C = O" decreased during cold glow discharge plasma oxygen treatment, indicating that plasma treatment increased cellulose crystallinity. The absorption peaks at 1605 and 1600 cm^{-1}, 1515 – 1505 cm^{-1}, and 1515 – 1505 cm^{-1} in all spectra were entirely attributable to aromatic ring vibration. The absorption peak at 1430 – 1425 cm^{-1} was responsible for CH_2 deformation in lignin in all absorption spectra. The peaks at 1330 and 1325 cm^{-1} might be amplified by lignin syringyl ring breathing. The C-O, C-C asymmetric vibration is responsible for the peak of around 1230 – 1220 cm^{-1} in celluloses and hemicelluloses. Apart from a maximum adherence to C-O, C-C of around 1235 cm^{-1}, was most visible in cold glow discharge plasma oxygen treatment of sisal fiber owing to cellulose oxidation. The reduction in aromatic and ketone compounds associated with bulk lignocellulosic absorption from fibers was primarily attributed to better plasma treatment parameters [49,50]."Two separate bands for C-C, C-O stretch as well as C-H, C-O deformations vibration at 1230 – 1220 cm^{-1} and 1085 – 1030 cm^{-1}, which appear to be characteristic of cellulose and lignin."The lack of a discernible peak at 1050 cm^{-1} shows that cellulose has been absorbed on the treated fiber's surface"[50]. The crystalline structure and morphology of cellulose have been related to the band at 1420–1430 cm^{-1}, whereas the amorphous area has been associated with the spectrum at 898 cm^{-1} [49,51]. It is possible to identify changes in this fingerprint region, showing that the fiber composition has improved.

This appears to be strong evidence that plasma exposure changes fiber shape. The Total Crystallinity Index, as well as Lateral Order Index values for banana fiber cold plasma oxygen at 80 W (30 min) and sisal fiber cold plasma oxygen at 80 W (30 min) treated with cold plasma oxygen, were the highest (1.281,0.891),(1.05,0.956), respectively, as shown in Table (2). Untreated banana fiber and sisal fiber exhibited the lowest Total Crystallinity Index and Lateral Order Index (1.130,0.9539) values (1.008,0.983), implying that their cellulose is made up of more amorphous domains

Table 2
IR crystallinity ratio of untreated banana and sisal fiber, Cold glow discharge plasma oxygen treated banana and sisal fiber 80 W (30 Min), and cold glow discharge plasma oxygen treated banana and sisal fiber 120 W (30 Min)

Sample	IR Crystallinity Ratio	
	Total Crystallinity Index [52–54]	Lateral order Index[52]
Untreated Banana Fiber	1.130	0.9539
Cold glow discharge plasma oxygen treated banana fiber 80 W (30 Min)	1.281	0.891
Cold glow discharge plasma oxygen treated banana fiber 120 W (30 Min)	1.19	0.926
Untreated Sisal Fiber	1.008	0.983
Cold glow discharge plasma oxygen treated Sisal fiber 80 W (30 Min)	1.05	0.956
Cold glow discharge plasma oxygen treated Sisal fiber 120 W (30 Min)	1.031	0.966

3.7 X-ray diffractograms (XRD)

The X-ray powder diffraction patterns for untreated banana fibers and cold glow discharge plasma oxygen-treated banana and sisal fibers at 80 W (30 min) as well as 120 W(30 min), are shown in Fig. 9(a), (b).rescpectively. Untreated banana and sisal fiber spectra show a substantial peak at 2θ values at 18.57°, 18.87° and a very strong peak at 22.14°, 22.63°, which correspond to 101 and 002 planes [55]. After exposing banana and sisal fibers to cold glow discharge plasma oxygen at plasma intensities of 80 W (30 min), 120 W (60 min) (30 min), there was a strong peak at 18.16°,18.14°,18.710°,18.725°, and a very strong peak at 22.69°,22.3°,22.609°,22.614°, which correspond to 101 and 002 planes, respectively. The greatest percentage crystallinity, crystallinity index, and amorphicity index values were obtained in banana fiber 80 W (30 min) treated with cold plasma oxygen (0.543, 54.37%, and 0.456), respectively). Table [3] depicts that the greatest values of % crystallinity, crystallinity index, and amorphicity index were reported in sisal fiber 80 W (30 min) treated with cold plasma oxygen (0.651,46.52% and 0.534). Since the surface of crystallites corresponding to amorphous cellulose section shrinkage reduced as crystallite size grew, the percent crystallinity, Crystallinity Index, and amorphicity index increased [55].

Table 3
XRD analysis of untreated banana and sisal fiber, Cold glow discharge plasma oxygen treated Banana and Sisal fiber 80 W (30 Min), and cold glow discharge plasma oxygen treated banana and sisal fiber 120 W (30 Min)

Fibers	Crystallinity Index (%) Proposed by Segal et.al. [56–58]		
	% Crystallinity	Crystallinity Index Cr.I.(%)	Amorphicity Index
Untreated Banana Fiber	0.62	38.73%	0.612
Cold glow discharge plasma oxygen treated banana fiber 80 W (30 Min)	0.543	54.37%	0.456
Cold glow discharge plasma oxygen treated banana fiber 120 W (30 Min)	0.494	49.49%	0.505
Untreated Sisal Fiber	0.6105	36.221%	0.6377
Cold glow discharge plasma oxygen treated sisal fiber 80 W (30 Min)	0.651	46.52%	0.534
Cold glow discharge plasma oxygen treated sisal fiber 120 W (30 Min)	0.643	44.56%	0.554

4. Conclusion

Tensile, % elongation, ILSS, flexural, force-extension curve, single fiber tensile test, FTIR, and XRD diffractogram characteristics of banana-sisal fiber-reinforced epoxy laminates significantly improved, denoting that cold glow discharge oxygen plasma treatment with banana, sisal fibers had been fully accountable. After cold glow discharge plasma oxygen treatment with plasma intensities of 80 W (30 min) and 120 W, the ultimate tensile strength as well as % Elongation break for banana- sisal fiber-reinforced epoxy laminate rose to 121.24 MPa,6.9 mm and 113.47 MPa,6.8 mm, respectively.This leads in improvements of 121.24%, 50.0%, and 101.366%, 47.82%, respectively. The flexural strength of the banana-sisal fiber-reinforced epoxy laminate improved to 74.91 MPa at 40% fiber volume after 30 minutes of treatment with a cold glow discharge plasma intensity of 80 W.Cold glow discharge plasma oxygen treated banana-sisal fiber-reinforced epoxy laminates with plasma intensities of 80 W(30 min) and 120 W(30 min) improve flexural strength properties by 132.27% and 124.34%, respectively, when compared to untreated banana-sisal fiber-reinforced epoxy laminates. As compared to pretreated banana-sisal fiber reinforced epoxy composites, interlaminar shear strength values for cold glow discharge plasma oxygen modified banana-sisal fiber reinforced epoxy composites employing plasma intensities of 80 W(30 min) and 120 W(30 min) increase significantly by 90.44% and 73.98%, respectively. The force-extension behavior of the banana-sisal fiber-reinforced epoxy laminate was considerably improved after being treated with cold glow discharge plasma oxygen.

Cold plasma oxygen treated banana-sisal fiber-reinforced epoxy laminates demonstrated increased force(N) values of 115.15% and 101.36%, respectively, were compared to untreated banana sisal fiber-reinforced epoxy laminates at plasma intensities of 80 W (30 min.) and 120 W (30 min.). The breaking load, tensile strength, along with % elongation break of the banana fiber after cold glow discharge plasma oxygen treatment with plasma intensities of 80 W (30 min) and 120 W (60 min) are 3.52N,53.31 Mpa,11.6 mm, and 3.18N,31.25 Mpa,9.3 mm respectively. After cold glow discharge plasma oxygen treatment with plasma intensities of 80 W (30 min) and 120 W (30 min), the breaking load, tensile strength, and % elongation break for sisal fiber is 4.14 N,72.344 Mpa,12.1 mm, and 3.76 N,46.775 Mpa,11.2 mm, respectively, after treatment with plasma intensities of 80 W (30 min) and 120 W (30 min). The greatest values for the “Total Crystallinity Index as well as Lateral Order Index” for banana fiber 80 W (30 min) treated with cold plasma oxygen were 0.936 and 1.285, respectively. The greatest values for the "Total Crystallinity Index" as well as "Lateral Order Index" for sisal fiber 80 W (30 min) treated with cold plasma oxygen were 0.956 and 1.05, respectively. The highest percent Crystallinity, Crystallinity Index, and Amorphicity Index values were 0.543, 54.37%, and 0.456 for banana fiber 80 W (30 min) treated with cold plasma oxygen, Sisal fiber 80 W (30 min) treated with cold plasma oxygen had percent Crystallinity, Crystallinity Index, and Amorphicity Index values of 0.651, 46.52 percent, and 0.534, respectively. indicating that hemicellulose and lignin were greatly reduced after cold glow discharge plasma oxygen treatment on banana fiber. Plasma treatment significantly increased the cohesive forces between fiber and matrix and boosted mechanical behavior.

Declarations

Acknowledgement Not applicable.

Authors’ Contributions Not applicable

Funding Finance

No funding was received by any of the authors on any level for research work to be carried.

Data Availability

The datasets supporting the conclusions of this article are included within the article and its additional files(ie. Tables,Line Figures)

Compliance with Ethical Standards

Conflict of Interest

The authors whose names are listed have NO affiliations with or involvement in any organization or entity with any financial interest (such as honoraria, educational grants, participation in speakers’ bureaus, membership, employment, consultancies, stock ownership, or other equity interest, and expert testimony or patent-licensing arrangements), or non-financial interest (such as personal or professional

relationships, affiliations, knowledge or beliefs) in the subject matter or materials discussed in this manuscript.

Ethics Approval

Not applicable.

Consent to Participate

Not applicable.

Consent for Publication

Not applicable.

Code Availability

Not applicable.

References

1. Tanasa, F., Z anoag a, M., Teaca, C., Nechifor,M., Shahzad, A, Modified hemp fibers intended for fiber-reinforced polymer composites used in structural applications:A review. I. Methods of modification. Polymer Composites 41, 5-31,2019
2. Martín del Campo, A., Robledo-Ortiz, J., Arellano,M., Jasso-Gastinel, C., Silva-Jara, J., López-Naranjo, E., Pérez-Fonseca, A. (2020),Glycidyl methacrylate as compatibilizer of poly(lactic acid)/nanoclay/agave fiber hybrid biocomposites: Effect on the physical and mechanical properties. Revista Mexicana de Ingeniería Química 19, 455-469,2020
3. Abdel-Fattah, E. Surface and thermal characteristics relationship of atmospheric pressure plasma treated natural luffa fibers. Eur. Phys. J. D 73, 71,2019, https://doi.org/10.1140/epjd/e2019-90281-3
4. Borsa J. 14-Antimicrobial natural fibres. In: Kozłowski RM, editor. Handbook of natural fibres. Woodhead publishing series in textiles. Woodhead Publishing, 2012. p. 428e66.
5. Leao AL, Cherian BM, De Souza SF, Kozłowski RM, Thomas S, Kottaisamy M. 9-Natural fibres for geotextiles. In: Handbook of natural fibres. Woodhead publishing series in textiles. Woodhead Publishing, 2012. p. 280e311. https://doi.org/10.1533/97808570955 10.2.280.
6. Pervaiz M, Panthapulakkal S, KC B, Sain M, Tjong J. Emerging trends in automotive light weighting through novel composite materials. Materials Sciences and Applications 2016,7:26e38. https://doi.org/10.4236/msa.2016.71004.
7. Dunne R, Desai D, Sadiku R, Jayaramudu J. A review of natural fibres, their sustainability and automotive applications. Journal of Reinforced Plastics and Composites 2016,35:1041e50 https://doi.org/10.1177/0731684416633898.

8. GomesM de A. Propriedades Mecaˆnicas de Compo´sitos polime´ricos reforc¸ados com fibras de folhas de abacaxizeiro. Universidade Estadual do Norte Fluminense Darcy Ribeiro, 2015.
9. Pritchard M, Sarsby RW, Anand SC. Handbook of technical textiles. In: Handbook of technical textiles, 2000. https://doi.org/10.1533/9781855738966.372.
10. Wambua, P, Ivens, J., Verpoest, I., Natural fibers: Can they replace glass in fiber-reinforced plastics? Compos. Sci. Technol. Vol. 63, pp. 1259-1264,2003
11. Huh, Yang Il, Bismark, Mensah, Kim, Sungjin, Lee, Hong Ki, and Na, Chang-Un, “Effects of Plasma Treatment on Mechanical Properties of Jute Fibers and Their Composites with Polypropylene,” Elastomers and Composites, vol. 47, no. 4, pp. 310–317, 2012
12. Yanjun Xie, Callum A.S. Hill, Zefang Xiao, Holger Militz, Carsten Mai, Silane coupling agents used for natural fiber/polymer composites: A review, Composites Part A: Applied Science and Manufacturing, Volume 41, Issue 7, pp. 806-819,2010, ISSN 1359-835X.
13. G. Borcia, C.A. Anderson, N.M.D. Brown, Surface treatment of natural and synthetic textiles using a dielectric barrier discharge, Surface and Coatings Technology, Vol. 201, Issue 6, pp. 3074-3081,2006, ISSN 0257-972.
14. Xiaowen Yuan, Krishnan Jayaraman, Debes Bhattacharyya, Effects of plasma treatment in enhancing the performance of wood fiber-polypropylene composites, Composites Part A: Applied Science and Manufacturing, Vol. 35, Issue 12, pp. 1363-1374,2004, ISSN 1359- 835X.
15. Jae-Ha Kim, Choong-Jae Lee, Kyung Deuk Min, Byeong-Uk Hwang, Dong Gil Kang, Don Hyun Choi, Jinho Joo, Seung-Boo Jung, Intense pulsed light surface treatment for improving adhesive bonding of aluminum and carbon fiber reinforced plastic (CFRP), Composite Structures, Vol. 258,pp113-364,2021.
16. E.M. Liston, The interfacial interactions, in G. Akovali (Ed.), Polymeric Composites,Kluwer Academic Publishers, Dordrecht, pp. 223–268,1993.
17. Brunengo, E., Conzatti, L., Utzeri, R., Vicini, S., Scatto, M., Falzacappa, E., Castellano, M., Stagnaro P., Chemical modification of hemp fibers by plasma treatment for eco composite based on biodegradable polyester. Journal of Materials Science, vol. 54, pp.14367-14377,2019.
18. De Melo, R., Marques, M., Navard, P., Duque, N., Degradation studies and mechanical properties of treated curauá fibers and microcrystalline cellulose in composites with polyamide 6. Journal of Composite Materials. vol. 51,pp. 1-9,2017.
19. Jang, J., Yang, H. The effect of surface treatment on the performance improvement of carbon fiber/polybenzoxazine composites. Journal of Materials Science, vol. 35,pp. 2297–2303 ,2000, https://doi.org/10.1023/A:1004791313979.
20. Rongzhi Li, Lin Ye, Yiu-Wing Mai, Application of plasma technologies in fiber-reinforced polymer composites: a review of recent developments, Composites Part A: Applied Science and manufacturing, Vol.28, Issue1, pp.73-86, 1997, ISSN1359-835X,
21. Karahan, H.A., Ozdogan, E. Improvements of surface functionality of cotton fibers by atmospheric plasma treatment. Fibers Polym. , 9, 21–26 ,2008.

22. Vander Wielen, L.C., Ostenson, M., Gatenholm, P., Ragauskas, A. Surface modification of cellulosic fibers using dielectric-barrier discharge. Carbohydr. Polym. , 65, 179–184.2006.
23. Yasuda H.,Plasma polymerization and plasma modification of polymer surfaces. In: Ebdon J.R., Eastmond G.C. (eds) New Methods of Polymer Synthesis. Springer, Dordrecht,1995, https://doi.org/10.1007/978-94-011-0607-8-5.
24. Mukhopadhyay, S., Pal, R., Narula, V., and Mayank, M.,. A study of interface behavior in sisal fibre composites—single fibre pull out test. Indian Journal of Fibre & Textile Research, 38 (1), pp. 87-91,2013.
25. Wang GJ, Liu YW, Guo YJ, Zhang ZX, Xu MX, Yang ZX. Surface modification and characterizations of basalt fibers with non-thermal plasma. Surf Coat Technol vol.201,pp. 6565–8,2007.
26. Zhou, Z., Liu, X., Hu, B., Wang, J., Xin, D., Wang, Z., and Qiu, Y., Hydrophobic surface modification of ramie fibers with ethanol pretreatment and atmospheric pressure plasma treatment, Surface and Coatings Technology, vol.205, pp. 4205–4210,2011.
27. Chen, C., Chen, J. C., and Yao, W. H., Argon plasma treatment for improving the physical properties of crosslinked cotton fabrics with di methylol dihydroxy ethylene urea acrylic acid, Textile Research Journal, vol.80 (8), pp. 675-682,2010.
28. Kamlangkla, K., Paosawatyanyong, B., Pavarajarn, V., Hodak, Jose H., and Hodak,Satreerat K,. Mechanical strength and hydrophobicity of cotton fabric after SF6 plasma treatment, Applied Surface Science, 256 (20), pp. 5888-5897,2010
29. Sun, D. and Stylios, G., Fabric surface properties affected by low temperature plasma treatment, Journal of Materials Processing Technology, 173 (2), pp. 172–177,2006
30. Gawish SM, Saudy MA, El-Ola SMA, Abou-El-Kheir A., The effect of low-temperature plasma for improving wool and chitosan-treated wool fabric properties. Journal of the TextileInstitutevol.102,pp.180-188,2011 doi:http://dx.doi.org/10.1080/00405000.2010.483836
31. Bozaci E, Sever K, Demir A, Seki Y, Sarikanat M, Ozdogan E. Effect of the atmospheric plasma treatment parameters on surface and mechanical properties of jute fabric. Fibers and Polymers vol.10,pp.781e6,2009 https://doi.org/10.1007/s12221-009-0781-6.
32. Kamlangkla, K., Paosawatyanyong, B., Pavarajarn, V., Hodak, Jose H., and Hodak,Satreerat K ,Mechanical strength and hydrophobicity of cotton fabric after SF6 plasma treatment, Applied Surface Science, 256 (20), pp. 5888–5897,2010.
33. Sun, D. and Stylios, G., Fabric surface properties affected by low temperature plasma treatment, Journal of Materials Processing Technology, 173 (2), pp. 172–177,2006
34. Balaji A, Karthikeyan B, Swaminathan J, Comparative mechanical, thermal, and morphological study of untreated and NaOH-treated bagasse fiber-reinforced cardanol green composites.Adv Compos Hybrid Mater .2(1):25–132,2019.
35. Jacob M, Thomas S, Varughese KKT, Mechanical properties of sisal/oil palm hybrid fiber reinforced natural rubber composites. Compos Sci Technol,64(7–8): 955–965,2004.

36. E.T.N. Bisanda, M.P. Ansell , The effect of silane treatment on the mechanical and physical properties of sisal-epoxy composites, Composites Science and Technology,41:165- 78,1991.
37. S. Marais, F. Gouanve, A. Bonnesoeur, J. Grenet, F. Poncin-Epaillard, C. Morvan, M. Métayer, Unsaturated polyester composites reinforced with flax fibers: effect of cold plasma and autoclave treatments on mechanical and permeation properties, Composites Part A: Applied Science and Manufacturing, 36: 975-986,2004, ISSN 1359-835X,https://doi.org/10.1016/j.compositesa.2004.11.008.
38. C.W.Kan,K. han,C.W.M. Yuen, M.H. Miao,Surface properties of low-temperature plasma treated wool fabrics,Journal of Materials Processing Technology,Vol. 83,Issues 1–3,pp.180-184,1998,ISSN 0924-0136.
39. Karmaker, A.C., Hoffmann, A., Hinrichen, G. Influence of water uptake on the mechanical properties of jute fiber-reinforced polypropylene.J. Appl. Polym. Sci. ,v ol.54, pp.1803–1807,1994
40. Mohanty, S., Nayak, S.K., Verma, S.K., Tripathy, S.S. Effect of MAPP as a coupling agent on the performance of jute–pp composites.J. Reinf. Plast. Compos.,vol. 23,pp. 625–637,2004
41. Yuan, X., Jayaraman, K. and Bhattacharyya, D.,Effects of plasma treatment in enhancing the performance of woodfibre-polypropylene composites,Compos. Part A-Appl S, Vol. 35,pp. 1363-1374, 2004.
42. Oliveira, F.R., Erkens, L., Fangueiro, R. et al. Surface Modification of Banana Fibers by DBD Plasma Treatment. Plasma Chem Plasma Process vol.32,pp. 259–273, 2012, https://doi.org/10.1007/s11090-012-9354-3
43. R. Morent, N. De Geyter, J. Verschuren, K. De Clerck, P. Kiekens, C. Leys,Non-thermal plasma treatment of textiles, Surface and Coatings Technology,Volume 202, Issue 14,pp. 3427-3449, 2008,ISSN 0257-972
44. Alexis Baltazar-y-Jimenez, Martina Bistritz, Eckhard Schulz, Alexander Bismarck,Atmospheric air pressure plasma treatment of lignocellulosic fibres: Impact on mechanical properties and adhesion to cellulose acetate butyrate,Composites Science and Technology,Vol. 68, Issue 1,pp. 215-227,2008,ISSN 0266-3538
45. Ebru Bozaci, Kutlay Sever, Mehmet Sarikanat, Yoldas Seki, Asli Demir, Esen Ozdogan, Ismail Tavman,Effects of the atmospheric plasma treatments on surface and mechanical properties of flax fiber and adhesion between fiber–matrix for composite materials,Composites Part B: Engineering,Vol. 45, Issue 1,pp. 565-572,2013ISSN 1359-8368,https://doi.org/10.1016/j.compositesb.2012.09.042
46. N. Médard, J.-C. Soutif, F. Poncin-Epaillard, CO2, H2O, and CO2/H2O Plasma Chemistry for Polyethylene Surface Modification, Langmuir 18 , pp. 2246–2253,2002,https://doi.org/10.1021/la011481i.
47. J.J.G. Van Soest, H. Tournois, D. De Vit, J.F.G. Vliegenhart, Short-range structure in (partially) crystalline potato starch determined with attenuated total reflectance Fourier transform IR spectroscopy. Carbohydrate Research vol. 279, pp. 201,1995.

48. Bergo, P. ,Carvalho, R. A., Sobral, P.J.A.. Physical properties of edible films based on cassava starch as affected by the plasticizer concentration. Packaging Technology and Science, vol 1, pp 1-2,2007.
49. Oh, S.Y., Yoo, D.I., Shin, Y., Seo, G. FTIR analysis of cellulose treated with sodium hydroxide and carbon dioxide. Carbohydr. Res., vol., 340, pp.417–428,2004.
50. Carrilo, F., Colom, X., Sunol, J.J., Saurina, J. Structural FTIR analysis and the thermal characterization of lyocell and viscose-type fibers. Eur. Polym. J. vol .40,pp. 2229–2234,2004 .
51. De Rosa IM, Kenny JM, Puglia D, Santulli C, Sarasini F. Morphological, thermal and mechanical characterization of okra (Abelmoschus esculentus) fibers as potential reinforcement in polymer composites. Composite Sci Technol vol.70(1), pp.116–22,2010.
52. Łojewska J, Miskowiec P, Łojewski T, Proniewicz LM. Cellulose oxidative and hydrolytic degradation: in situ FTIR approach, Polym Degrad Stabil,vol.88(3),pp.512–20,2005.
53. De Rosa IM, Kenny JM, Maniruzzaman M, Moniruzzaman Md, Monti M, Puglia D, Santulli C, Sarasini F. Effect of chemical treatments on the mechanical and thermal behavior of okra (Abelmoschus esculentus) fibers. Composite Sci Technol, vol.71(2), pp. 246–54,2011.
54. Hon, D.N.S. Cellulose: a random walk along its historical path. Cellulose 1,pp. 1–25,(1994), https://doi.org/10.1007/BF00818796
55. Nelson, M.L., O'Connor, R.T. Relation of certain infrared bands to cellulose crystallinity and crystal lattice type. Part I. Spectra of types I, II, III and of amorphous cellulose. J. Appl. Polym. Sci. ,vol. 8, pp.1311–1324,1964
56. Oh, S.Y., Yoo, D.I., Shin, Y., Seo, G. FTIR analysis of cellulose treated with sodium hydroxide and carbon dioxide. Carbohydr. Res.,vol., 340, pp.417–428,2004
57. Carrilo, F., Colom, X., Sunol, J.J., Saurina, J. Strucutral FTIR analysis and the thermal characterization of lyocell and viscose-type fibers. Eur. Polym. J. vol .40,pp. 2229–2234,2004
58. Wada, M., Okano, T. Localization of Iα and Iβ phases in algal cellulose revealed by acid treatments. Cellulose , vol.8,pp. 183–188,2001
59. Popescu, M.-C., Popescu, C.-M., Lisa, G., Sakata, Y, Evaluation of morphological and chemical aspects of different wood species by spectroscopy and thermal methods. J. Mol. Struct.vol.988,pp. 65–72,2011
60. Gumuskaya, E., Usta, M., Kirei, H. ,The effects of various pulping conditions on crystalline structure of cellulose in cotton linters. Polym. Degrad. Stab.,vol. 81, pp.559–564,2003
61. Kim, U,J. Eom, S.H. Wada, M. Thermal decomposition of native cellulose: Influence on crystallite size. Polym. Degrad. Stab.,vol. 95,pp. 778–781,2010

Figures

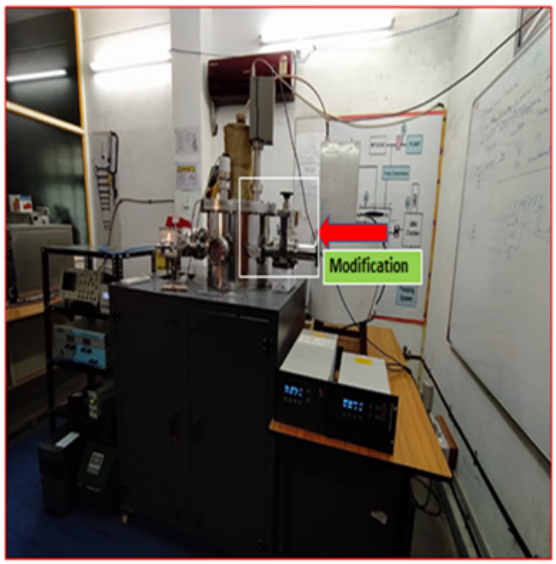

Figure 1

Experimental set up for Producing Glow Discharge Plasma

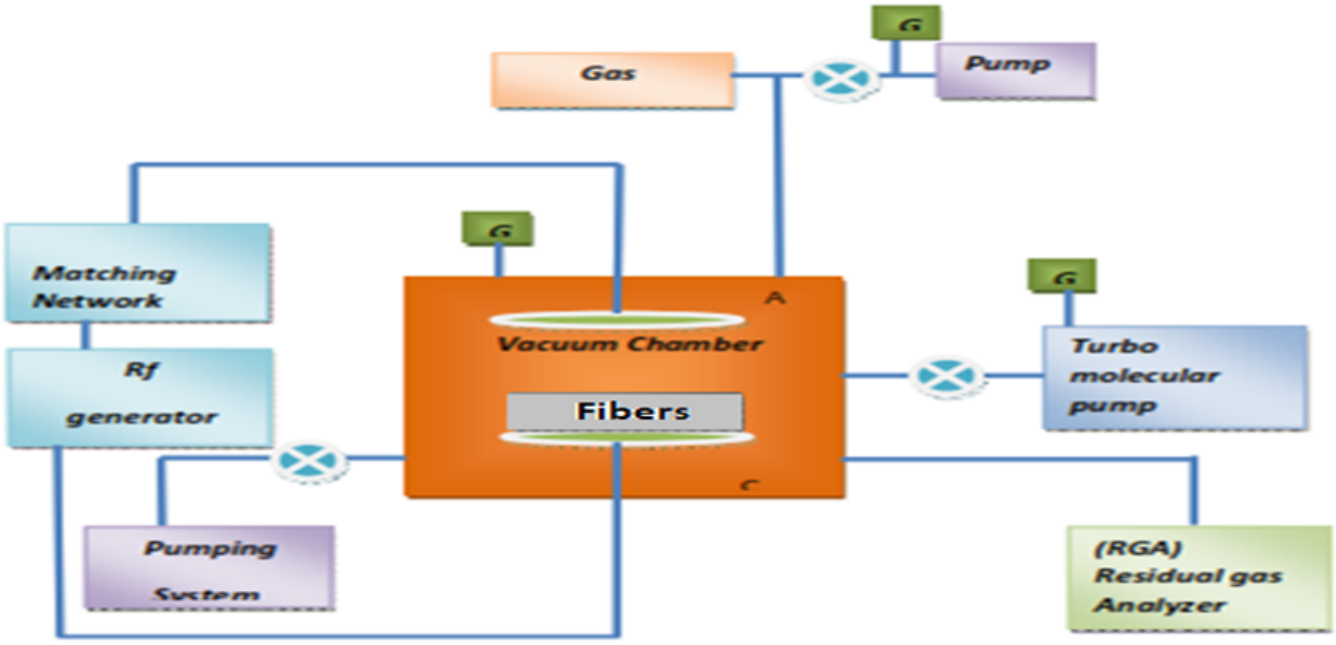

Figure 2

Flowchart for Producing Cold Glow Discharge Plasma

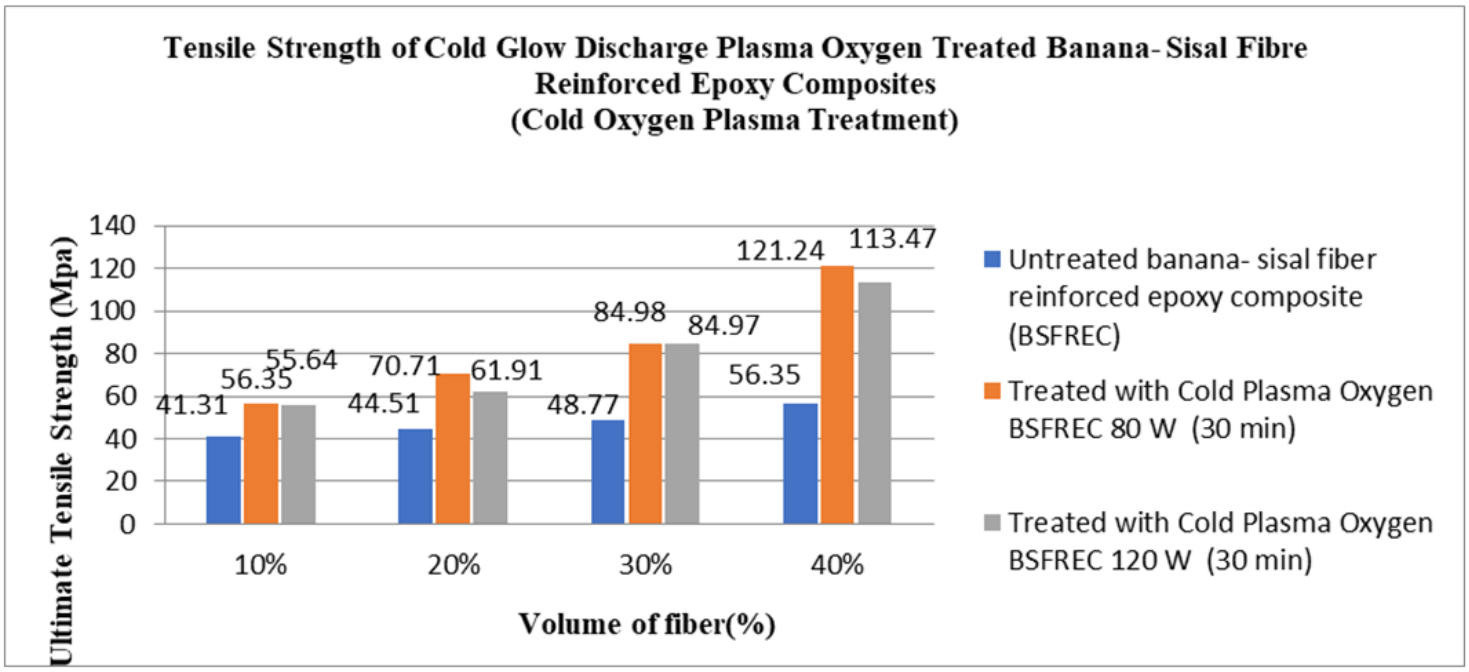

Figure 3

Impact of cold glow discharge plasma oxygen modification on the tensile strengths banana - sisal fiber-reinforced epoxy laminates

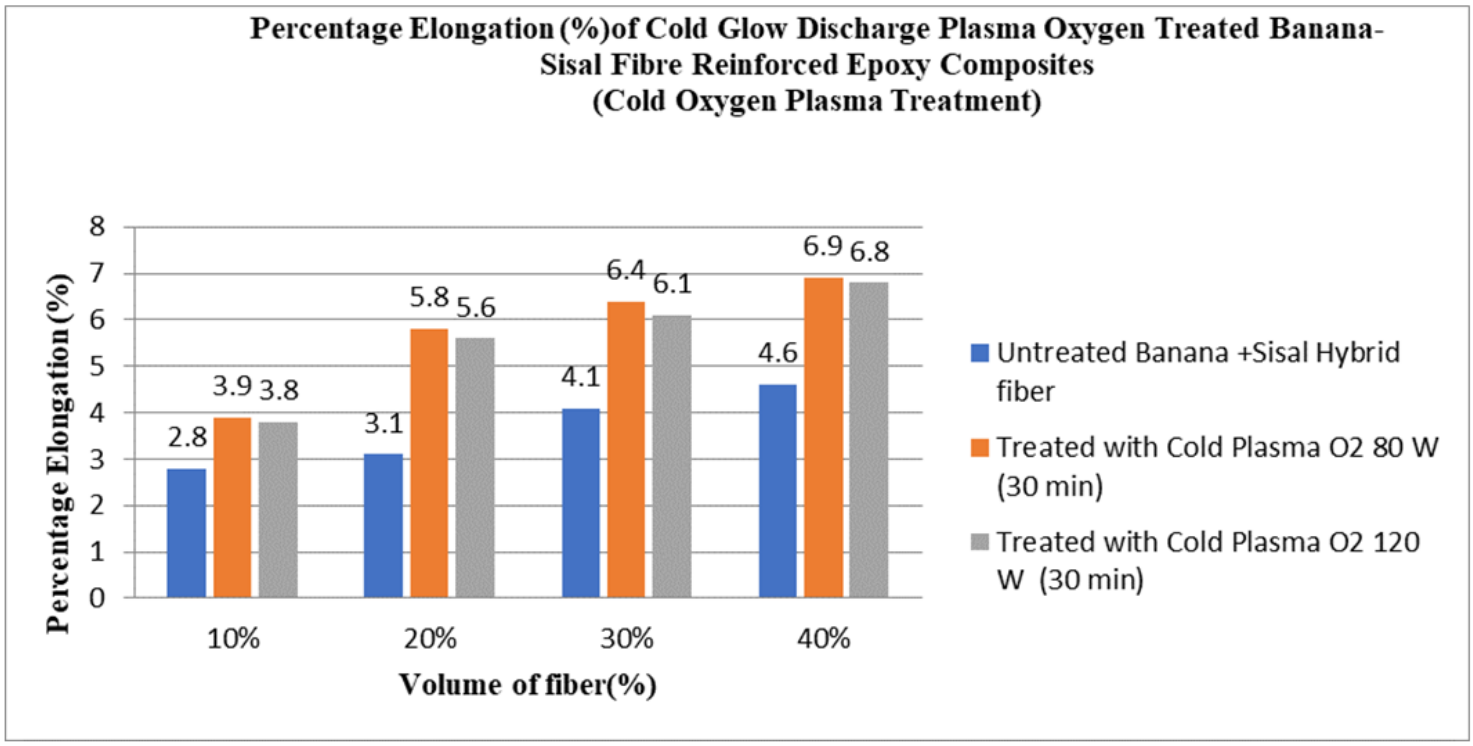

Figure 4

Impact of cold glow discharge plasma oxygen modification on the % elongation banana -sisal fiber-reinforced epoxy laminates

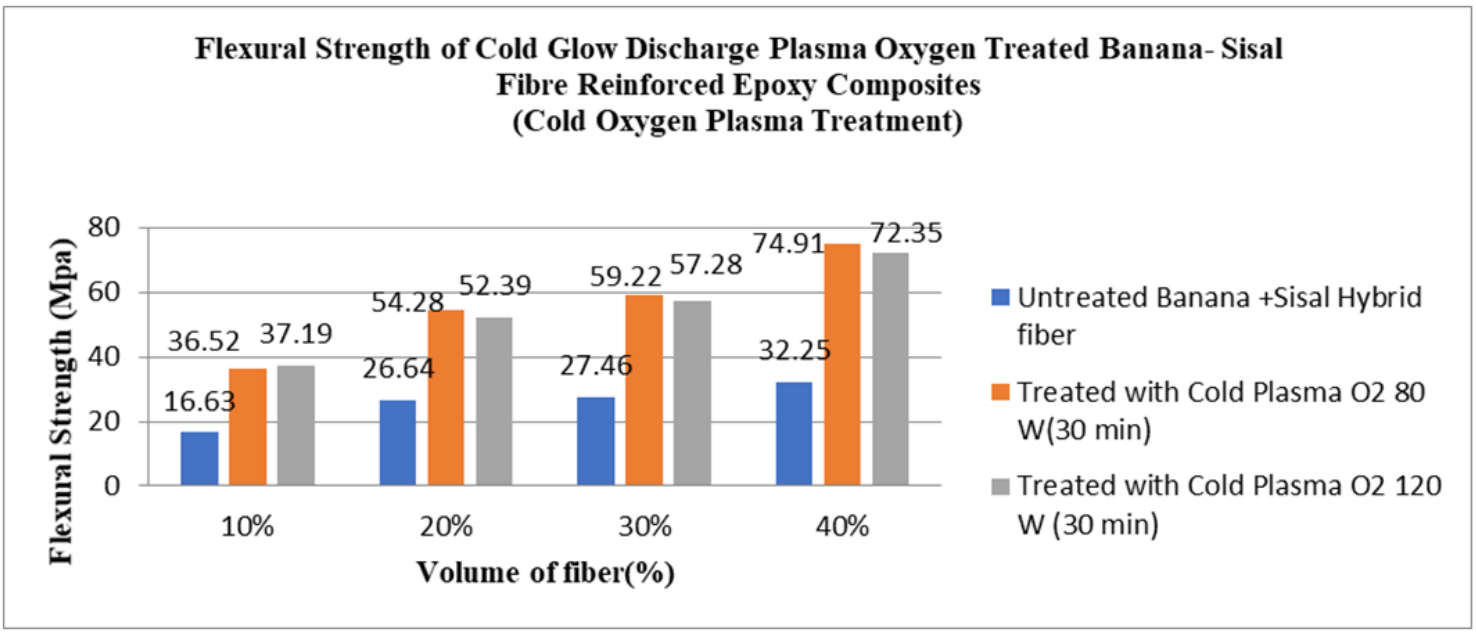

Figure 5

Impact of cold glow discharge plasma oxygen treatment on the flexural strengths of untreated as well as cold glow discharge of plasma-treated banana- sisal fiber-reinforced epoxy laminates

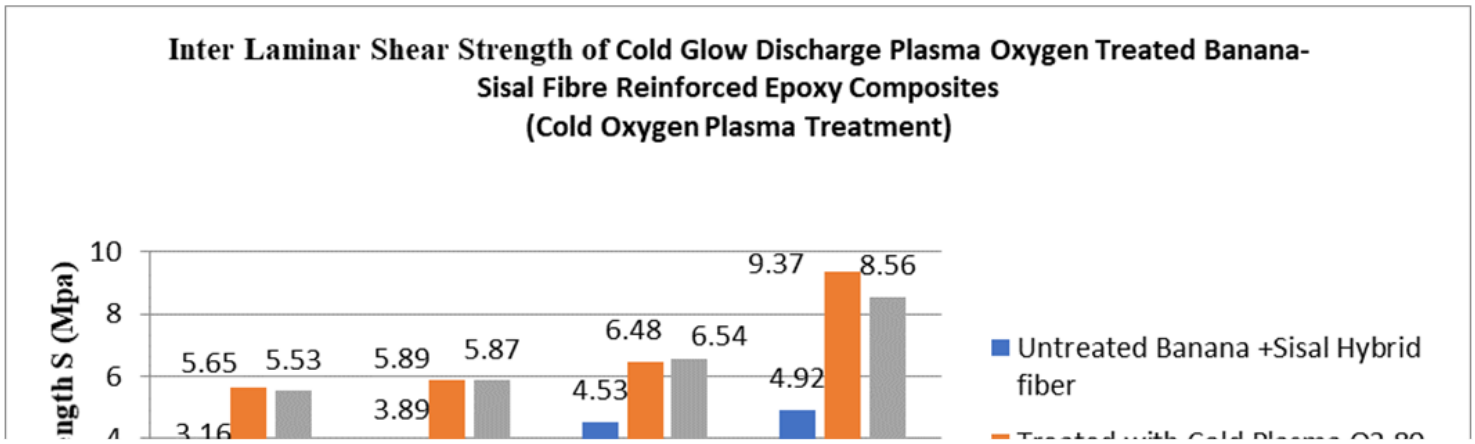

Figure 6

Impact of cold glow discharge plasma oxygen treatment on the ILSS strengths of pretreated as well as cold glow discharge of plasma-treated banana sisal fiber -reinforced epoxy composites

Figure 7

(a).The force-displacement curve for banana-sisal fiber-reinforced epoxy laminates

(b). Impact of cold glow discharge plasma oxygen modification on the Force- displacement curve for cold glow discharge of plasma oxygen modification banana- sisal fiber-reinforced epoxy laminates.

(c). Impact of cold glow discharge plasma oxygen modification on the force-displacement curve for cold glow discharge of plasma oxygen modification banana- sisal fiber-reinforced epoxy laminates

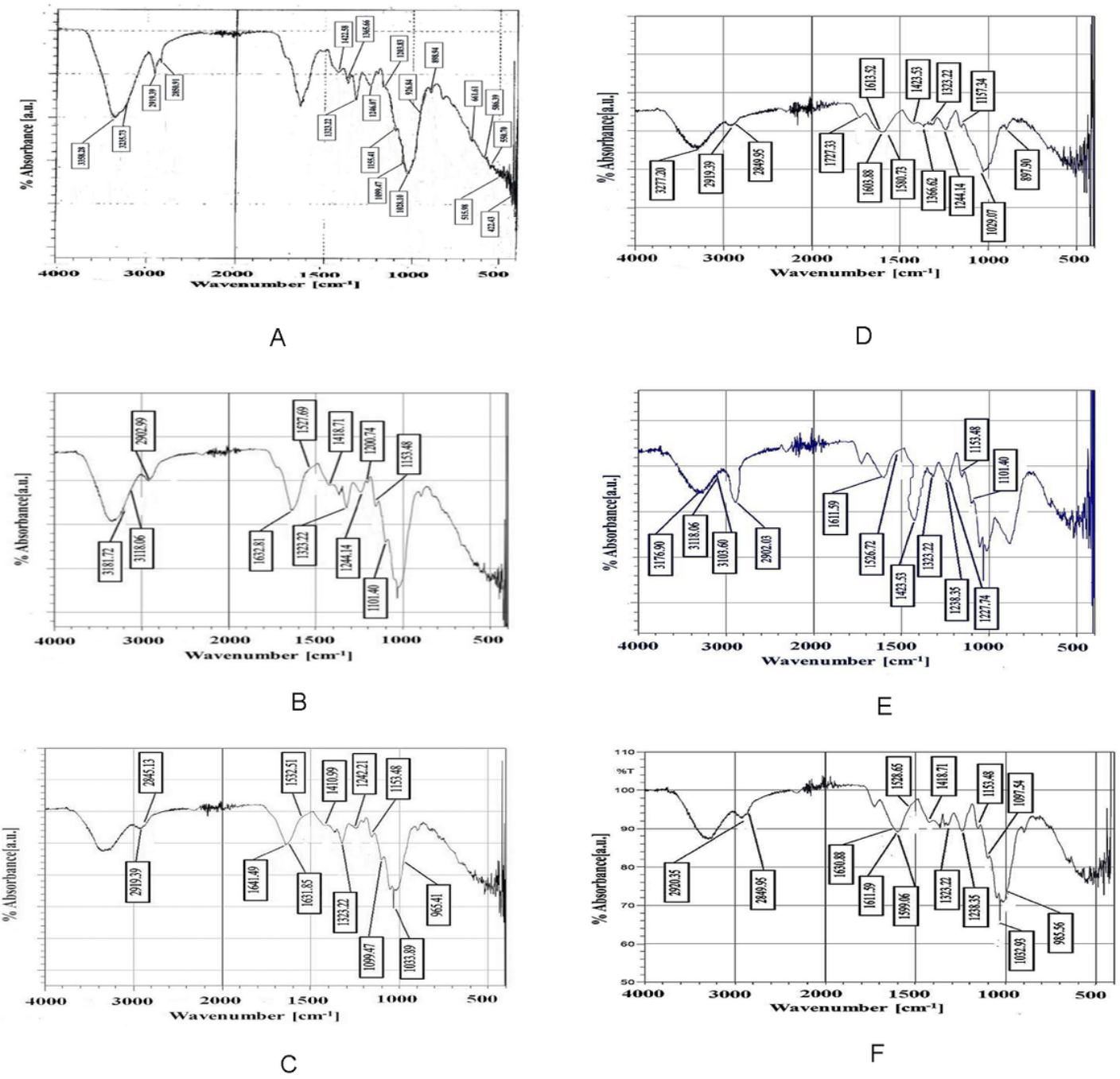

Figure 8

(a). IR spectrum of untreated banana fiber

(b). IR spectrum of cold glow discharge plasma oxygen treated banana fiber 80 W (30 min)

(c). IR spectrum of cold glow discharge plasma oxygen treated banana fiber 120 W (30 min)

(d). FTIR spectra of untreated sisal fiber

(e). FTIR spectra of cold glow discharge plasma oxygen treated sisal fiber 80 W (30 min)

(f). FTIR spectra of cold glow discharge plasma oxygen treated sisal fiber 120 W (30 min)

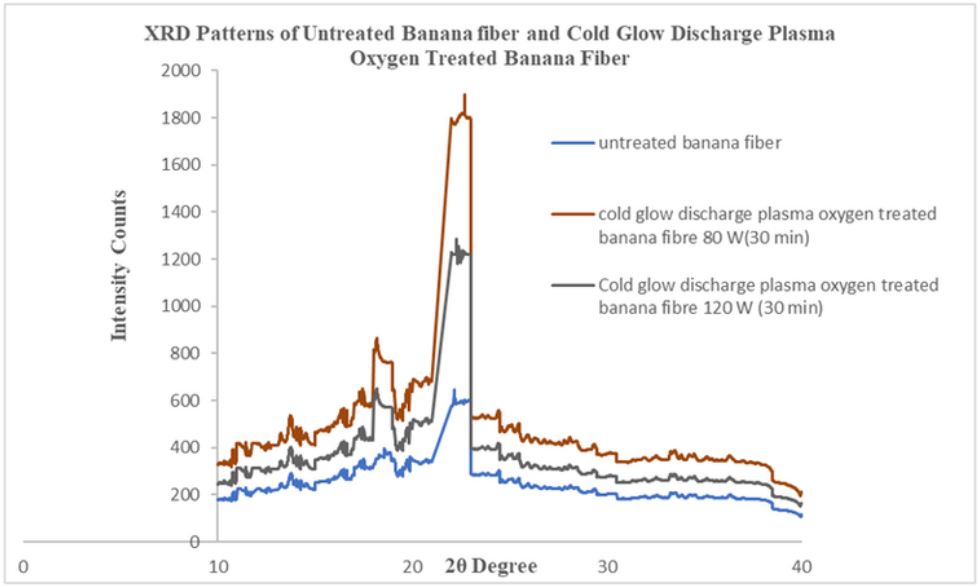

A

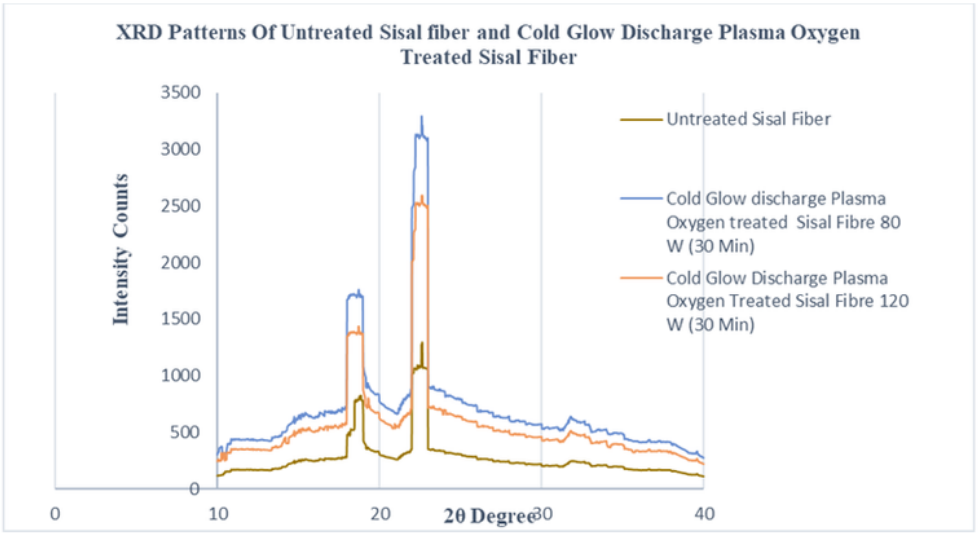

B

Figure 9

(a) XRD diffractogram for untreated banana fiber, Cold glow discharge plasma oxygen treated banana fiber 80 W (30 Min), and cold glow discharge plasma oxygen treated banana fiber 120 W (30 Min)

(b) XRD diffractogram of untreated sisal fiber, Cold glow discharge plasma oxygen treated sisal fiber 80 W (30 Min), and cold glow discharge plasma oxygen treated sisal fiber 120 W (30 Min)